

Diffusion and hydrodynamic dispersion with the lattice Boltzmann method

A. Caì

*IBM European Center for Scientific and Engineering Computing, Via del Giorgione 159, 00147 Rome, Italy
and Department of Hydraulic Engineering, University of Catania, Viale A. Doria 6, 95125 Catania, Italy*

S. Succi

IBM European Center for Scientific and Engineering Computing, Via del Giorgione 159, 00147 Rome, Italy

A. Cancelliere

Department of Hydraulic Engineering, University of Catania, Viale A. Doria 6, 95125 Catania, Italy

R. Benzi

Physics Department, University of Rome "Tor Vergata," Via E. Carnevale, 00173 Rome, Italy

M. Gramignani

Department of Hydraulic Engineering, University of Catania, Viale A. Doria 6, 95125 Catania, Italy

(Received 9 August 1991)

A simple reinterpretation of the lattice Boltzmann equation is presented that allows it to track passive scalar dynamics in grossly irregular geometries without adding any new ingredient to the basic hydrodynamic algorithm. The scheme is numerically demonstrated for two representative test cases: diffusion in two-dimensional fractal media and Taylor hydrodynamic dispersion.

PACS number(s): 47.55.Mh, 02.70.+d, 51.10.+y

INTRODUCTION

Diffusion and hydrodynamic dispersion in random media is a subject of wide interdisciplinary concern, ranging from electron transport in disordered media to pollutant dispersion in subterranean flows to fluid injection in oil reservoirs. This broad range of application motivates the strong interest in the search for new and efficient numerical methods to solve the dynamics of a passive scalar, i.e., a quantity moving with the fluid flow except for possibly the effect of diffusion in grossly irregular geometries.

In this respect, a numerical tool, known as the lattice Boltzmann equation (LBE), has been proposed recently, which seems to be particularly well placed to handle the aforementioned situations. The basic merits of this technique are an easily handling of complex boundary conditions as well as its ideal amenability to parallel computing.

The LBE has already been proved effective in the calculation of transport properties of three-dimensional random media [1], such as the permeability of a bed of penetrable spheres, as well as in the study of the complex dynamics of multiphase flows in porous media [2].

In this paper, we show that a simple reinterpretation of the LBE permits an extension of its range of applicability to problems of tracer diffusion and hydrodynamic dispersion in grossly irregular geometries. Since the original hydrodynamic algorithm is left practically untouched, this opens up a set of important applications which can be handled within this framework of a unique computational tool.

PASSIVE SCALAR DYNAMICS WITH THE LBE

The lattice Boltzmann equation is a finite-difference equation governing the evolution of a discrete set of mean populations $f_i(\mathbf{x}, t)$ $i = 1, b$, representing the probability of finding a particle with speed \mathbf{c}_i at node \mathbf{x} at time t . Although originally derived upon ensemble averaging of an underlying lattice-gas automaton dynamics, it has been recognized that LBE can be viewed as a self-standing kinetic model, which converges to the Navier-Stokes equations in the hydrodynamical limit. Formally, the LBE takes the following form:

$$f_i(\mathbf{x} + \mathbf{c}_i, t + 1) - f_i(\mathbf{x}, t) = \sum_j A_{ij} (f_j - f_j^{\text{eq},2}) \quad (1)$$

where A_{ij} is the scattering matrix mediating collisions between populations f_i and f_j , and $f_j^{\text{eq},2}$ is the equilibrium distribution function expanded up to second-order terms in the macroscopic flow field in order to retain adjectic effects:

$$f_j^{\text{eq},2} = \frac{\rho}{16} \frac{D^2}{2c^4} G(\rho) \left[c_{j\alpha} c_{j\beta} - \frac{c^2}{D} \delta_{\alpha\beta} \right] u_\alpha u_\beta, \quad (2)$$

where

$$G(\rho) = \frac{2}{3} \frac{1 - \rho/12}{1 - \rho/24}$$

is a factor due to the lack of Galilean invariance and ρ is the density. The discrete speeds \mathbf{c}_i are chosen to belong to a 4D face-centered hypercube (FCHC), which is known to ensure the correct symmetries needed in order

for Eq. (1) to converge to the Navier-Stokes equations in the hydrodynamical limit [3]. In the FCHC lattice, each node is surrounded by 24 neighbors defined by the cyclic permutation of the quadruplet $(\alpha, \alpha, 0, 0)$ with $\alpha = \pm 1$ (see Fig. 1).

The convergence of Eq. (1) to the Navier-Stokes equation is best highlighted by projection upon the eigenvectors of the collision matrix A_{ij} [4]. This yields a set of partial differential equations for the hydrodynamical fields, i.e., the fluid density $\rho = \sum_i f_i$, current $J_\alpha = \sum_i f_i c_{i\alpha}$, and momentum flux tensor

$$S_{\alpha\beta} = \sum_i f_i \left[c_{i\alpha} c_{i\beta} - \frac{c^2}{D} \delta_{\alpha\beta} \right],$$

which take the following form:

$$\begin{aligned} \partial_t \rho + \partial_\alpha J_\alpha &= 0, \\ \partial_t J_\alpha + \partial_\alpha \frac{\rho}{2} + \partial_\beta S_{\alpha\beta} &= 0, \quad \alpha, \beta = 1, 4, \\ \partial_t S_{\alpha\beta} + \partial_\alpha J_\beta + \partial_\beta J_\alpha &= \lambda (S_{\alpha\beta} - S_{\alpha\beta}^{\text{eq}}), \end{aligned} \quad (3)$$

where $S_{\alpha\beta}^{\text{eq}} = \rho G(\rho) [u_\alpha u_\beta - (u^2/4)\delta_{\alpha\beta}]$. It is readily checked that in the adiabatic limit ($\partial_t \ll \lambda$), these equations reduce to the Navier-Stokes equations with a viscosity $\nu = -\frac{1}{6}(1/\lambda - 1/2)$, $-2 < \lambda < 0$, being the leading nonzero eigenvalue of the collision matrix A_{ij} .

It should be noted that these equations have been obtained by starting from the differential form of Eq. (1). This implies that their validity is restricted to those situations where hydrodynamic quantities do not vary appreciably over a few lattice spacing units.

Projection upon three-dimensional space results in the quenching of the self-transport of the fourth component of the current, i.e., $J_4 \partial J_4 / \partial x_4 = 0$, so that J_4 is convected as a passive scalar by the three-dimensional flow, with a diffusivity $D = \nu$, i.e., at a unit Schmidt number.

Thus, the 24-speed FCHC model can be used to track a passive scalar in a three-dimensional flow with no further addition of degrees of freedom. The same reasoning, reported in two dimensions, leads to two passive scalars, J_3 and J_4 , conveyed by the two-dimensional flow

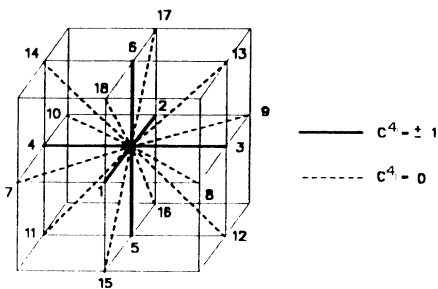


FIG. 1. Three-dimensional projection of the 4D face-centered-hypercube. Direct links (1,2,3,4,5,6) carry two degenerate populations, while diagonal links (7,8,9,10,11,12,13,14,15,16,17,18) carry only one.

$\mathbf{J} = (J_1, J_2)$.

In the following we shall restrict our attention to the case of a single passive scalar in 2D, so that we impose $J_3 \neq 0$ and $J_4 = 0$. The most natural way to impose $J_4 = 0$ is to assume the same values for the populations propagating along opposite directions with respect to x_4 . It is readily checked that this leaves us with only 18 distinct populations, six becoming degenerate (those along thick links in Fig. 1). The current field is then defined as

$$J_\alpha = \sum_{i=1}^{18} p_i c_{i\alpha} f_i, \quad \alpha = 1, 3, \quad (4)$$

where p_i is the number of populations propagating along the direction c_i , i.e., $p_i = 1$ for diagonal links and $p_i = 2$ for nearest-neighbor communications. From the point of view of the practical implementation, the collision step stays exactly the same as for 3D hydrodynamics (with no tracers), while the streaming phase reduces to 18 propagations along 9 distinct directions. As a result, the inclusion of the tracer dynamics requires only few minor changes in the streaming and reflection sections of the code.

APPLICATIONS

We will now exhibit two applications, anomalous diffusion in fractal media and Taylor hydrodynamic dispersion in a two-dimensional channel, which are particularly meaningful in terms of proving the validity of the LBE method as a numerical tracker of passive scalars in complex geometries. All the numerical simulations have been performed on the IBM 3090 vector multiprocessor at IBM ECSEC.

Diffusion in self-similar structures is known to be anomalous; the mean-squared displacement from the origin R^2 of a point particle walking inside the fractal does not scale linearly with time (as in the case of normal diffusion). Instead, a power law $R^2 \sim t^{2\nu}$, with an exponent ν smaller than 0.5, is found. Anomalous diffusion is tantamount to a scale-dependent diffusion coefficient D . In fact, according to the definition of D as the limit at large t of the ratio R^2/t , one readily obtains $D \sim R^{2-1/\nu}$. It is then clear that an accurate evaluation of the anomalous exponent is highly prized in terms of assessing the transport properties of random media.

Unfortunately, the exact computation of ν by analytical means can only be performed in a very limited number of cases. One such case is provided by the Sierpinski gasket, the fractal obtained by repeatedly cutting a triangle in four subtriangles of halved side and leaving the central one off (see Fig. 2). For this structure, an exact decimation procedure leads to the following result (in two-dimensions) [5]: $\nu = \ln 2 / \ln 5$. This exact result can then be used as a test case for the LBE code. A set of numerical simulations has been performed with two different resolutions: 128^2 and 256^2 , corresponding to six and seven generations, respectively.

For each of these cases, five runs have been performed

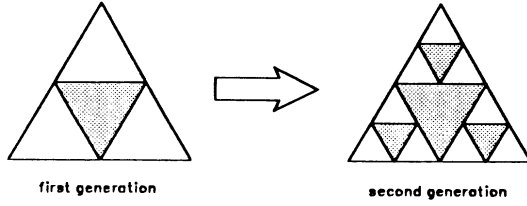


FIG. 2. One step of the recursive procedure generating the Sierpinski gasket.

by varying the initial position (x_0, y_0) of the tracer $C(x, y, t=0) = C_0 \delta(x - x_0) \delta(y - y_0)$. The flow setup is as follows. The fluid density is $\rho = 7.87$, corresponding to a fluid viscosity $\nu = 0.032$, the macroscopic flow speed is zero, and the tracer mass is $C_0 = 0.4$. The mean-square displacement is then computed as

$$R^2 = \frac{1}{C_0} \int [(x - x_0)^2 + (y - y_0)^2] C(x, y) dx dy, \quad (5)$$

where

$$C(x, y) \equiv J_3 = \sum_{i=1}^{18} p_i c_{i3} f_i$$

is provided by the numerical simulation. The results, displayed in Figs. 3 and 4 clearly show that despite some statistical fluctuations, the exact exponent is well recovered on the average.

This result was not granted *a priori* because of lack of convergence to a continuum fluid limit can be expected in the neighborhood of the corners of the fluid triangles. These points represent a sort of geometrical singularity where communication between fluid regions is inhibited. In practice, this singularity is handled by treating the corners as fluid sites, thereby allowing tracer particles to diffuse throughout the whole fluid medium. More precisely, for a better compatibility with the FCHC topology, the Sierpinski lattice used in the simulations is con-

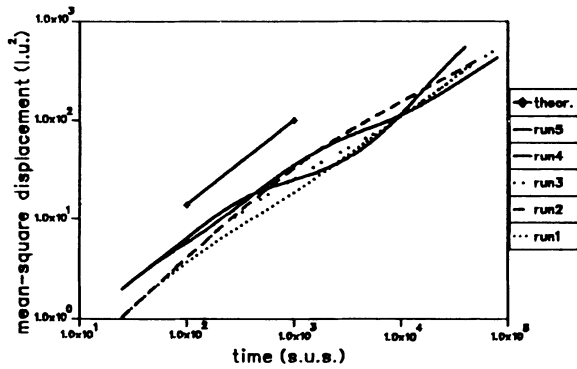


FIG. 3. Mean-square displacement in square lattice units in the 128×128 grid Sierpinski gasket as a function of time in simulation unit steps. The straight line represents the exact result, while the others refer to numerical simulations with five distinct initial conditions.

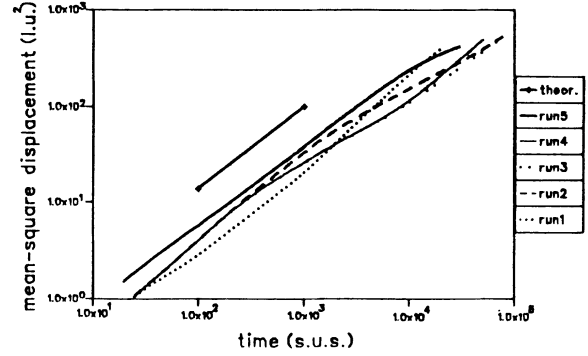


FIG. 4. The same as Fig. 3, with a doubled resolution (256×256) grid.

structed by cutting squares into four subsquares of half-side length and tagging the lower left as the solid one. Communication between fluid subregions is then ensured by particle flights proceeding along the diagonal links. The present results indicate that the gross transport coefficients are insensitive to these microgeometrical details, as witnessed by the fact that the two resolutions, 128^2 and 256^2 , yield essentially the same result.

As a second test case we address the case of Taylor hydrodynamic dispersion. In this case, in addition to diffusing, the tracer is also convected by the fluid flow (a parabolic Poiseuille profile between two parallel plates). The asymptotic analysis of Taylor hydrodynamic dispersion in a two-dimensional channel of width H leads to the following formula for the longitudinal diffusion coefficient ([6] and references therein):

$$D_{\parallel} = D + \frac{H^2 U_m^2}{210D} = D \left[1 + \frac{Pe^2}{210} \right] \quad (6)$$

where $U_m = \frac{2}{3} U_{\max}$ is the average flow speed and $Pe = HU_m / D$ is the flow Péclet number. This formula is based on the assumption that diffusion across the channel

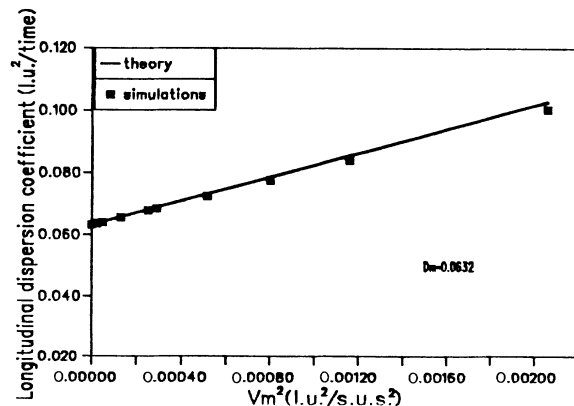


FIG. 5. Longitudinal diffusion coefficient as a function of the square flow speed. The solid line corresponds to Eq. (6), while the dots refer to the numerical results. The measure was taken after 5000 time steps. Channel grid 16×1024 .

has come to an equilibrium. In addition, this equilibrium must be such that concentration C does not display any appreciable variation along the vertical coordinate y . More precisely, by defining

$$\bar{C}(x) = \frac{1}{H} \int_0^H C(x,y) dy, \quad \Delta C(x,y) = C(x,y) - \bar{C}(x) \quad (7)$$

the formula (6) holds in the limit $\Delta C / \bar{C} \ll 1$. This condition is better and better fulfilled as the Péclet number tends to zero.

The LBE code has been tested against Eq. (6) for a number of different values of the diffusion coefficient D , the channel width H , and length L . The tracer is initialized as $C(x,y,t=0) = C_0 \delta(x-L/2)$ with $C_0 = 0.5$. The other parameters are $\rho = 7.87$ and $\nu = 0.063$.

A typical result, referring to the case $D = 0.0632$, $H = 16$, $L = 1024$ is displayed in Fig. 5, in which the ratio $D_{\parallel} \equiv (\langle \xi^2 \rangle - \langle \xi \rangle^2) / (2t)$, where $\xi = x - L/2$, has been computed with the code. As a first remark, we see that

the quadratic dependence on the flow speed is perfectly recovered, as well as the value of the molecular diffusion coefficient $D = 0.063$ in the limit of vanishing flow speed.

The numerical values of D_{\parallel} appear slightly smaller (a few percent) than the theoretical ones. This slight discrepancy may be attributed to the fact that the assumption on which Eq. (6) is based is less and less valid as the Péclet number increases.

In summary, the present results indicate that the LBE is a suitable computational tool for tracking passive scalar dynamics in hydrodynamics flows taking place in grossly irregular geometries.

ACKNOWLEDGMENT

A.C., A.C., R.B., and M.G. wish to acknowledge IBM Direzione Ricerca Scientifica e Tecnologica for financial support and computational facilities.

-
- [1] A. Cancelliere, C. Chang, E. Foti, D. Rothman, and S. Succi, *Phys. Fluids* **2**, 2085 (1990).
 [2] A. Gunstensen, D. Rothman, S. Zaleski, and G. Zanetti, *Phys. Rev. A* **43**, 4320 (1991).
 [3] D. d'Humières, P. Lallemand, and U. Frisch, *Europhys. Lett.* **2**, 291 (1986).

- [4] M. Vergassola, R. Benzi, and S. Succi, *Europhys. Lett.* **13**, 411 (1990).
 [5] S. Havlin and D. Ben-Avraham, *Adv. Phys.* **36**, 696 (1987).
 [6] C. Baudet, J. P. Hulin, D. d'Humières, and P. Lallemand, *Phys. Fluids* **1**, 507 (1989).

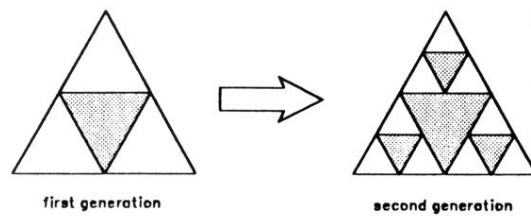


FIG. 2. One step of the recursive procedure generating the Sierpinski gasket.